Three-Dimensional Chord Distribution Function SAXS Analysis of the Strained Domain Structure of a Poly(ether ester) Thermoplastic Elastomer

N. Stribeck*,† and S. Fakirov‡

Institut für Technische und Makromolekulare Chemie, Universität Hamburg, 20146 Hamburg, Germany; and University of Sofia, Laboratory on Structure and Properties of Polymers, 1126 Sofia, Bulgaria

Received April 6, 2001; Revised Manuscript Received August 20, 2001

ABSTRACT: The nanostructure deformation mechanism of a predrawn and annealed poly(ether ester) (PEE) thermoplastic elastomer comprising poly(butylene terephthalate) as hard segments and poly(ethylene glycol) as soft segments of a weight ratio 57/43 was studied by means of synchrotron radiation. For this purpose a recently proposed method by Stribeck for extraction of the topological domain structure information contained in the small-angle X-ray scattering (SAXS) patterns was applied to patterns observed as a function of elongation of PEE when measured in the strained and in the relaxed state after straining. The SAXS fiber diagram as a whole was transformed into a three-dimensional chord distribution function (CDF) with fiber symmetry. Assignment of the observed peaks to the various structural characteristics of the PEE is suggested.

Introduction

A serious disadvantage of the classical projection analysis is the laborious multistage background subtraction that must be carried out for each projected scattering curve. Moreover, the projection reflects only a partial aspect of the structure (Bonart's *longitudinal* and *transverse structures*, respectively).[1]

A recently proposed method[2] allows one to extract and visualize topological domain structure information contained in scattering patterns from small-angle scattering (SAS) without complex pretreatment. Multidimensional, noisy raw data can be processed. Such data are for instance accumulated in the field of materials research from short-time exposed in situ SAXS experiments with synchrotron radiation. The result is a multidimensional intersect or chord distribution function (CDF), which is defined as the Laplacian of the correlation function. Moreover, it is equivalent to the autocorrelation of the gradient of the electron density.

Thus, the construction of the CDF is based on the well-known notion of displacing a "ghost" morphology with respect to the real structure and recording a scalar value as a function of the displacement vector in physical space. Because of the properties of the Laplacian operator, a peak will be observed in the CDF whenever a domain surface element of the ghost touches a domain interface element of the real structure. Then the strength of the observed peak is proportional to the scalar product of the two unit normal vectors to the domain interface elements (and several other quantities). This means that domain surfaces penetrating each other at right angles will not contribute, whereas the maximum peak will be observed whenever the domain surfaces in touch are oriented parallel to each other. For this extreme case, two subcases must be distinguished. In the first case, the real structure as well as the ghost structure have their "electron rich" phase on the same side of the interface. Then the peak has all the characteristics of a repeat unit in a series of particles ("lattice": single or multiple long period, respectively) and is attributed negative sign. In the second case the peak has the characteristics of a particle ("domain": solid or compound domain, respectively) and is given a positive sign.

The realization of this approach poses a major problems, namely, to extend the laborious multistage background determination established in SAXS curve analysis (Ruland[3]) to two-dimensional (2D) SAXS images. The proposed solution of this problem is based on spatial frequency filtering of the scattering intensity data. According to it the background to be subtracted from the small-angle scattering pattern is formed from its own low spatial frequencies. Noise may be removed by suppressing high spatial frequencies. In the frequency band in between, information on the domain structure of the nanocomposite appears.[2]

The technique is, in particular, adapted to the analysis of the nanoscale structure of samples with fiber symmetry, such as of polymer fibers or of strained elastomers. Multidimensional relations among morphological components become apparent in real space and help to elucidate the nature of the processes governing formation and change of structure on the nanometer scale.

The present note reports on results of application of the recently proposed method[2] for extraction of strained domain structure information from SAXS pattern of poly(ether ester) thermoplastic elastomer using synchroton radiation as a continuation of our systematic studies on the strain-induced structural changes in PEE thermoplastic elastomers.[4−8]

Experimental Section

Material. Bristles of diameter of about 1 mm were prepared by means of melt extrusion of thermoplastic elastomers of poly(ether ester) (PEE) type[6−8] comprising poly(butylene terephthalate) (PBT) as hard segments and poly(ethylene glycol)

* To whom all correspondence should be addressed. E-mail: Norbert.Stribeck@desy.de.
† Universität Hamburg.
‡ University of Sofia.

10.1021/ma010603a CCC: $20.00
Published on Web 09/29/2001

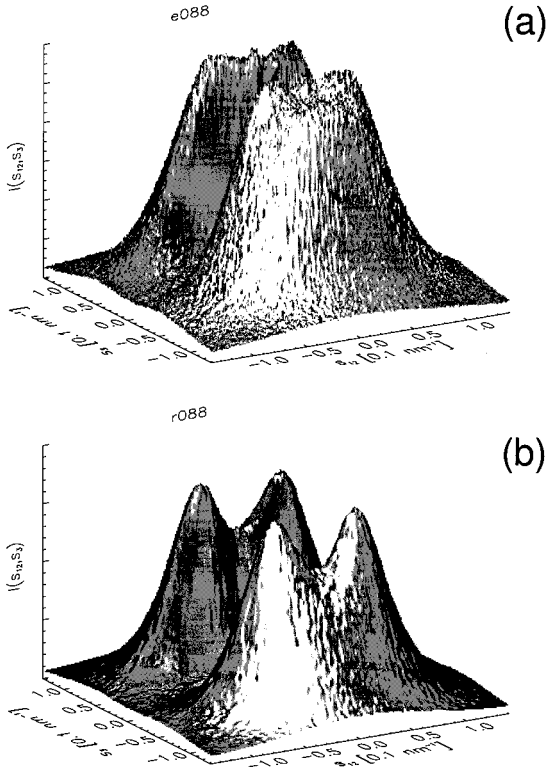

Figure 1. 2D scattering patterns of PEE sample 57/43 (1000): (a) at $\epsilon = 88\%$; (b) relaxing from $\epsilon = 88\%$.

(PEG) as soft segments. PEE contains PEG with molecular weight 1000 in a weight ratio 57/43 (PBT/PEG 1000). This isotropic (according to X-ray tests) bristles were drawn at room temperature until the entire sample underwent neck formation, corresponding to a draw ratio $\lambda = l/l_o = 5$. The drawn material exhibited a reversible deformation (ϵ) at room temperature of about 50%. Here and hereafter the elongation ϵ is defined as $\epsilon = 100\,(l - l_0)/l_o$, with l_o the initial and l the actual filament length, measured between marks placed close to the irradiated zone of the sample. The drawn bristles were annealed with fixed ends in a vacuum at 170 °C for 6 h and thereafter used for the SAXS measurements.

Small-Angle X-ray Scattering Measurements. Synchrotron radiation generated at the beamline A2 of HASYLAB in Hamburg, Germany, was applied. The sample-to-detector distance was set to 1800 mm. 2D SAXS patterns were registered on image-plates exposed between 2 and 5 min. An area of 900 × 900 pixels, each with a size of 176 μm × 176 μm, was read out and used for data evaluation. A stretching machine mounted in the pathway of the X-ray beam allowed for controlled elongation of the PEE sample in an ϵ range from 0 to 200%. After increasing the strain to the next step, a scattering pattern was recorded under stress. Then the bristle was released, the image plate was exchanged, and a pattern in the relaxed state was taken followed by a measurement under stress at higher deformation.

Results and Discussion

Figure 1 shows the original scattering patterns of the two samples discussed here. In the strained state (Figure 1a) a "six-point pattern" is indicated. During relaxation (Figure 1b) a well-separated four-point pattern is observed. The complete straining series has been subject to two earlier publications.[6,8] After having studied the evolution of domain thickness in straining direction only, now the first steps of a multidimensional analysis are demonstrated. According to the new method[2] the scattering intensity is first projected on to the

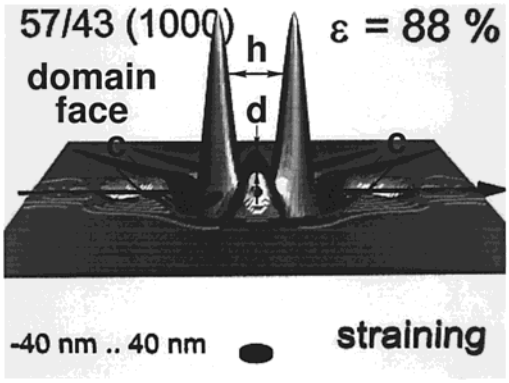

Figure 2. 3D chord distribution (CDF) of PEE sample 57/43 (1000) at $\epsilon = 88\%$ viewed from its domain face: (h) domain height peaks; (d) domain diameter peaks; (c) interdomain correlation peaks.

representative plane of the fiber diagram and, second, multiplied by $4\pi s^2$ (proportional to the square of the distance from its center). This operation is equivalent to the Laplacian in the physical space. Third, a background is constructed from the pattern itself by low-pass filtering (first-order Butterworth filter). Fourth, the background is subtracted, and fifth, a two-dimensional Fourier transform is applied. The result is a 3D chord distribution.

A first result is shown in Figure 2. The fiber axis x_3 is indicated by the bold arrow in the base plane. Obviously, the surface representing the CDF comprises both positive and negative values which are forming peaks. In the chosen representation, the positive peaks can be observed clearly. Here the correlations between beginning and end of each individual domain are forming strong peaks, which are marked in the figure. The letter h marks the highest peaks that characterize the height of the soft and the hard domains. Because of considerable width of the soft and hard domain distributions, the corresponding peaks are merged. d points at two peaks on the equator that are shaped by the diameter distribution of the cylindrical domains. Under oblique angle with respect to the fiber axis, four interdomain correlation peaks (c) show that the closest neighbors are not in line with the fiber axis; they form a macrolattice with short-range correlation. These peaks carry a positive sign, because they count chords starting from the "front" surface of a cylinder to the "back" surface of its closest neighbor. The long periods are indicated by the deepest valleys in the surface and are best viewed after turning it upside down (Figure 3). From this point of view, it becomes obvious that the correlation of entities having a long period in straining direction (a) is less pronounced than that of the entities tilted away with respect to the fiber axis (b). Again, the nanostructure exhibits only short-range correlations among the domains. Moving a domain in the fiber direction, one meets another "front" surface at a distance of about 24 nm (a) (Figures 3 and 6), but the domain behind this surface is of random thickness only. On the other hand, the movement of the domain in the oblique direction (b) reveals a better-defined morphological feature. In addition to a new interface (i.e., a long period) b, a domain of rather well-defined extension (cf. Figures 2 and 5c) is found behind this front interface.

After releasing the strain, another scattering pattern is taken. The corresponding 3D CDF is shown in Figure 4. In this representation the long period peaks are well

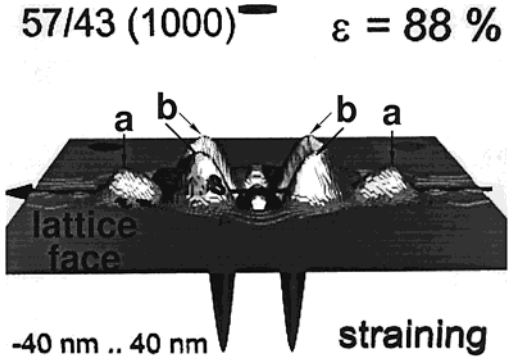

Figure 3. 3D CDF of PEE sample 57/43 (1000) at $\epsilon = 88\%$ viewed from its lattice face: (a) long period to the next neighbor in the fiber direction; (b) stronger long period to the next neighbor under oblique angle.

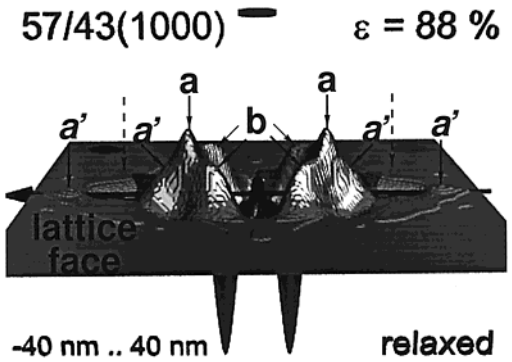

Figure 4. 3D CDF of PEE sample 57/43 (1000) relaxing from $\epsilon = 88\%$ viewed from its lattice face: (a) strongest long period to the next neighbor in the fiber direction (11 nm) (dashed arrows indicate the former position of this peak in the strained state); (a′) best correlated long period (17 nm) in the fiber direction and ist second order; (b) nearly constant long period to the next neighbor under oblique angle (satellite domains).

separated, revealing a very well expressed eight-point pattern ($2 \times a + 4 \times b + 2 \times a'$ for the first time. Further, compared to the strained state, the positions of the long period under oblique angle b (Figure 4) remain relatively constant, suggesting that many of the cylindrical domains are surrounded by identical satellites that are firmly coupled to their center. Such an ensemble has some of the properties of a stack from tilted lamellae. Here, in addition, a relatively rigid intradomain bridge appears to couple the central domain to its satellites. A speculative morphological explanation for the observed rigid domain coupling could resort on the notion of a compound hard domain made both from amorphous and crystalline zones. From the point of view of small-angle scattering these zones would be ascribed to different domains because of different electron density.

A first step from interpretation to analysis of the 3D chord distributions can be done by the help of contour plots. Figure 5 shows the contour plot of the surface shown in Figure 2. From the peak positions an average domain height of 7 nm and a domain diameter of 7 nm can be determined. Concerning the determination of the domain heights and their distributions, a more exact method takes the CDF along its central, vertical line and fits it by a one-dimensional stacking statistics.[8] But this method is neither able to gain information on the lateral extension of the domains nor able to describe the correlations among the domains under an oblique angle

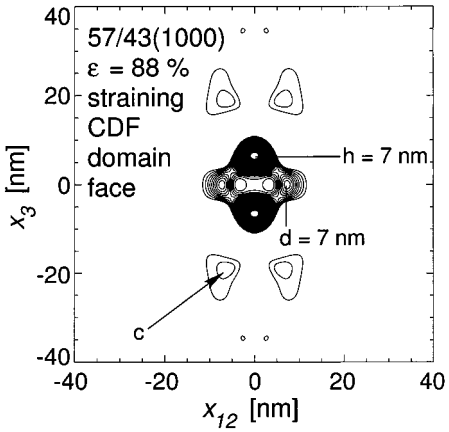

Figure 5. Contour plot corresponding to Figure 2 with peak positions indicating height (h), diameter (d), and correlation (c) of domains.

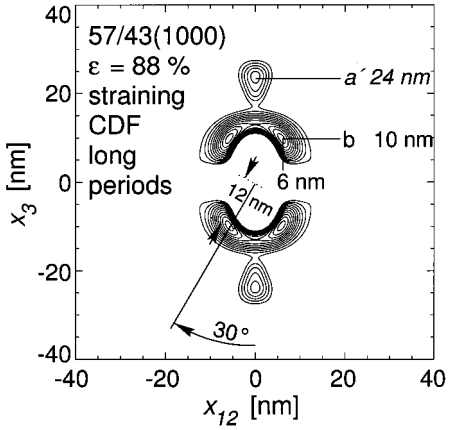

Figure 6. Contour plot corresponding to Figure 3 of the long period peaks with marks demonstrating a simple extraction of structural parameters.

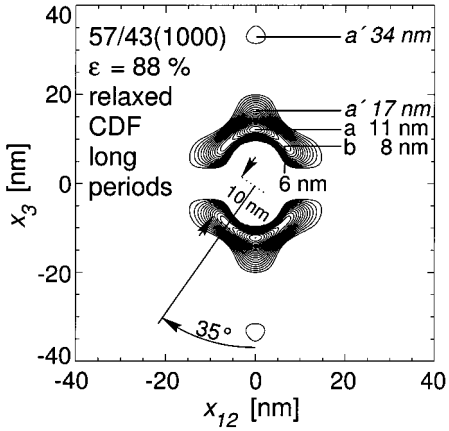

Figure 7. Contour plot corresponding to Figure 4 of the long period peaks with marks demonstrating a simple extraction of structural parameters.

with respect to fiber axis. Figures 6 and 7 show contour plots of the negative peaks (long periods) in the CDF for the strained and the relaxed state, respectively, and the numerical data which, to a first approximation, can be extracted from the peak positions.

Let us compare the nanostructure in the fiber direction in the strained state to the morphology after releasing the strain. The most prominent change is in the strong long period a′ on the meridian. From a strong

peak at 24 nm it decreases to 17 nm. Only in the relaxed state a clear second order is observed, revealing a microfibrillar component with medium range order in the fiber direction. Because of the fact that the second order is clearly visible, this component can be described as a system of several well-defined hard domain cylinders arranged in a row oriented in the fiber direction.

Conclusions

Summarizing, we would like to stress that the increased quality of SAXS data recorded in current experiments has encouraged us to freshen Bonart's method of projection analysis which has been dormant for decades. This technique was coupled to existing methods for the quantitative analysis of one-dimensional structure scattering or particle scattering. The obtained quantitative results elucidate structuring processes on the nanometer scale, taking place during elongation and relaxation of the elastomers. For instance, the process governing failure of the hard domains can be determined for different grades of poly(ether ester)s. With the extension toward the multidimensional chord distribution, an approach promising a full data analysis appears to be found. The CDF can be interpreted more clearly in terms of the underlying nanoscale morphology than the scattering pattern itself. Nevertheless, a full analysis by suitable multidimensional model functions is considered a challenge.

Acknowledgment. This study has been supported by the Bilateral Cooperation Program between the University of Hamburg, Germany, and the University of Sofia, Bulgaria, which is funded by the DAAD (German Academic Exchange Service). SAXS investigations were supported by HASYLAB, Hamburg, Germany. S.F. expresses his warmest thanks to the Alexander von Humboldt Foundation for the "Humboldt Research Award" enabling his stay at the Institute for Composite Materials Ltd at the University of Kaiserslautern, Kaiserslautern, Germany, where this paper was finalized. The hospitality of the latter is also greatly appreciated.

References and Notes

(1) Bonart, R. *Kolloid Z. Z. Polym.* **1966**, *211*, 14−33.
(2) Stribeck, N. *J. Appl. Crystallogr.* **2001**, *34*, 496−503. http://www.iucr.org/cgi-bin/paper?ks0053
(3) Ruland, W. *J. Appl. Cryst*, **1971**, *4*, 70−73.
(4) Fakirov, S.; Fakirov, C.; Fischer, E. W.; Stamm, M. *Polymer* **1991**, *32*, 1173−1180.
(5) Fakirov, S.; Fakirov, C.; Fischer, E. W.; Stamm, M. *Polymer* **1992**, *33*, 3818−3827.
(6) Stribeck, N.; Sapundjieva, D.; Denchev, Z.; Apostolov, A. A.; Zachmann, H. G.; Stamm, M.; Fakirov, S. *Macromolecules* **1997**, *30*, 1329−1339.
(7) Stribeck, N.; Fakirov, S.; Sapundjieva, D. *HASYLAB Annu. Rep.* **1998**, 531−532.
(8) Stribeck, N.; Fakirov, S.; Sapundjieva, D. *Macromolecules* **1999**, *32*, 3368−3378.

MA010603A